

Metabolic characterization of engineered P. fluorescens PfO-1 coexpressing E. coli NADH insensitive cs and S. typhimurium sodium citrate transporter or B. subtilis magnesium citrate transporter operon



CHAPTER 4

4 INTRODUCTION

4.1 Citrate transport in plants, fungi, and bacteria

Secretion of metabolites across plasma membrane requires the presence of transport mechanisms. Organic acids cannot pass the membrane barrier by simple diffusion and hence transport proteins are required for secretion of citrate, oxalate and succinate. The efflux of organic anions e.g., malate, citrate, or oxalate is an important mechanism for Al resistance in cereal and noncereal species. Overexpression of gene, encoding a transporter reported to enhance citrate efflux and Al tolerance in several plant species (**Table 4.1**). Members of the multidrug and toxin compound extrusion (MATE) family of proteins control Al-activated citrate efflux from barley (*Hordeum vulgare*) and sorghum (*Sorghum bicolor*). MATE proteins are widely present in bacteria, fungi, plants, and mammals (Omote et al. 2006), but there is no apparent consensus sequence conserved in all MATE proteins. MATE proteins are proposed to transport small, organic compounds (Omote et al., 2006). In contrast to MATE genes in the bacterial and animal kingdom, plants contain more MATE-type transporters (Furukawa et al., 2007). These proteins are characterized by having 400 to 700 amino acids with 12 transmembrane helices.

Table 4.1: Enhanced organic acid efflux by transporter gene expression (Ryan et al., 2011)

Transporter gene	Transgenic strategy	Proposed mechanism
Al ³⁺ activated malate transporter (TaLMT1)	Arabidopsis gene expressed in Arabidopsis, wheat gene expressed in wheat and Arabidopsis	Enhanced malate efflux
Multidrug and toxic compound efflux gene (MATE) called Frd3	Arabidopsis gene expressed in Arabidopsis	Enhanced citrate efflux

Multidrug and toxic compound efflux gene (MATE) (HvAACT1)	Barley gene expressed in tobacco plants	Enhanced citrate efflux
H ⁺ pyrophosphatase AVP1	Over-expression of endogenous gene in Arabidopsis, tomato and rice	Enhanced organic acid efflux
Multidrug and toxic compound efflux gene (SbMATE)	Sorghum gene expressed in Arabidopsis Atalmt1 mutant	Enhanced citrate efflux
Al ³⁺ activated malate transporter (HvALMT1)	Barley gene expressed in barley	Enhanced malate efflux
Multidrug and toxic compound efflux gene (ZmMATE1)	Maize gene expressed in arabidopsis	Enhanced citrate efflux

Citrate secretion is a common characteristic feature of many anamorphic fungal species like *Aspergillus* and *Penicillium* (Burgstaller, W., 1993; 2005). Total intracellular citrate level in *A. niger* is between 2 - 30 mM. In *P. simplicissimum*, citrate levels are between 10 - 50 mM during the growth in batch cultures and between 20 mM and 60 mM in chemostat cultures (Gallmetzer and Burgstaller, 2001). More than 1 M citrate secretion is achieved in *A. niger* in improved biotechnological production processes (Netik et al., 1997; Ruijter et al., 2002). Citrate overflow mechanism in *A. niger* is very different from bacteria and is pH dependent (must be < 3). In addition to pH, other factors *viz* carbon source type and concentration, N source and P concentration, excessive aeration and Mn²⁺ limiting condition are contribute towards citrate secretion in fungus (Mlakar and Legisa, 2006). An efflux of protons was postulated as the main charge-balancing ion flow in *Penicillium cyclopium* (Roos and Slavik, 1987).

Very few bacterial species like *Corynebacterium*, *Arthrobacter*, *Brevibacterium*, *Bacillus sp.*, *Bradyrhizobium japonicum*, and *Citrobacter koseri* are known to secrete or accumulate citrate at levels much lower than fungi (Gyaneshwar et al., 1998; Khan et al., 2006). A proton efflux could either be coupled directly to citrate secretion via a

[Genetic engineering of *P. fluorescens* for enhanced citric acid secretion]

citrate/proton symport similar to the secretion of lactate together with protons in *Escherichia coli* and *Lactobacillus lactis* (Konings et al., 1992). The membrane potential generating secondary transporters involved in malolactic (MelP) and citrolactic (citP) fermentation process are well reported in several lactic acid bacteria. The nature of transporters differ from “usual” secondary transporters in two aspects: (i) they translocate net negative charge across the membrane, and (ii) they catalyze efficient heterologous exchange of two structurally related substrates (Bandell et al., 1997). The electrochemical gradient of protons across the cytoplasmic membrane is a major store of free energy in the bacterial cell. Usually, the proton motive force (pmf) is generated by translocation of protons against the gradient across the cell membrane which results in the two components of the pmf, a membrane potential and a pH gradient. Proton pumping is catalyzed by primary transport systems at the expense of some source of chemical energy or light.

E. coli cannot utilize citrate as a sole source of carbon and energy (Dimroth, 1987; Kastner 2000). On the other hand, the facultative anaerobic bacteria *Klebsiella pneumoniae* and *Salmonella typhimurium* and many other species of the *Enterobacteriaceae* can grow aerobically or anaerobically, utilizing citrate as the sole carbon source. Most of the bacteria have transport proteins in the cytoplasmic membrane that mediate the transport of citrate. The carriers belong to the class of secondary transporters that use the free energy stored in transmembrane electrochemical gradients of ions to drive the transport of the substrates. The citrate transporter CitH of *K. pneumoniae* is driven by the proton motive force (van de Rest et al., 1991) while the transporters CitS and CitC of *K. pneumoniae* and *Salmonella* serovars are driven by both pmf and sodium, respectively. CitM of *Bacillus subtilis* is driven by magnesium ion motive force (Ishiguro et al., 1992; Lolkema, 1994; Boorsma et al., 1996). *Klebsiella pneumoniae citS* gene is expressed during anaerobic growth on citrate (Bott et al., 1995; Dimroth and Thomer, 1986).

Mechanistically these transporters catalyze coupled translocation of citrate and H⁺ and/or Na⁺ and Mg²⁺ (symport). A special case are the citrate carriers of lactic acid bacteria that take up citrate by an electrogenic uniport mechanism or by exchange with lactate, a

product of citrate metabolism (citrolactic fermentation) (Marty-Teyssset et al., 1996, Ramos et al., 1994). These citrate transporters are involved in secondary metabolic energy generation (Konings et al., 1995). In contrast with most citrate transporters, a member of the CitMHS family characterized from the soil bacterium *Bacillus subtilis*, transport citrate in complex with a bivalent metal ion. This facilitates the utilization of citrate which is available in the metal-ion-complexed state. The best-characterized members of the family are BsCitM and BsCitH. The former transports citrate in complex with Mg^{2+} and is the major citrate-uptake system during growth on citrate under aerobic conditions (Korm et al., 2000; Yamamoto et al., 2000; Li et al., 2002; Warner et al., 2002).

These Secondary transporters of the bacterial CitMHS family fall under the group of 2-hydroxycarboxylate transporter (2HCT) family. The 2HCT family of secondary transporters contains 54 unique members that are all found in the bacterial kingdom. The well characterized members of the family are transporters for citrate, malate and lactate, substrates that contain the 2-hydroxycarboxylate motif, hence the name of the family. The transporters are either H^+ or Na^+ symporters or they catalyze exchange between two substrates. Na^+ coupled citrate transporters like CitS of *Klebsiella pneumoniae* and CitC of *Salmonella enterica* found in the γ subdivision of the phylum Proteobacteria are involved in the fermentative degradation of citrate to acetate and carbon dioxide yielding ATP. Citrate is cleaved by citrate lyase yielding acetate and oxaloacetate, which is decarboxylated yielding pyruvate. The latter step results in the transmembrane pH gradient. Secondary transporters are widely distributed in nature and they come in a great genetic and structural diversity, probably reflecting many different translocation mechanisms. (Table 4.2, Lolkema, 2006).

Table 4.2: Characterized members of the 2HCT family (Lolkema, 2006).

Transporter	Bacterium	Substrates	Transport mode	Function
CitS	<i>Klebsiella pneumoniae</i>	citrate	Na ⁺ symport	citrate fermentation
CitC	<i>Salmonella typhimurium</i>	citrate	Na ⁺ symport	citrate fermentation
CitW	<i>Klebsiella pneumoniae</i>	citrate, acetate	exchange	citrate fermentation
MleP	<i>Lactococcus lactis</i>	malate, lactate	exchange	malolactic fermentation
CitP	<i>Leuconostoc mesenteroides</i>	citrate, lactate	exchange	citrolactic fermentation
CimH	<i>Bacillus subtilis</i>	citrate, malate	H ⁺ symport	unknown
MalP	<i>Streptococcus bovis</i>	malate	H ⁺ symport	malate fermentation
MaeN	<i>Bacillus subtilis</i>	malate	Na ⁺ symport	growth on malate

4.1.1 Structural Model of 2-HCT transporters

The transporters in the 2HCT family are integral membrane proteins consisting of about 440 amino acid residues (Lolkema, 2006). The core of the structure is formed by two homologous domains that are connected by a large hydrophilic loop that resides in the cytoplasm. The domains contain 5 transmembrane segments (TMSs) each and they have opposite orientations in the membrane. They are likely to originate from a duplication of an internal gene fragment coding for an odd number of TMSs. In the structural model of the transporters in the 2HCT family, the loops between the 4th and 5th TMSs in each domain fold back in between the TMSs and form so called re-entrant or pore loops (**Fig. 4.1**). The pore loop in the N-terminal domain (region VB) enters the membrane-embedded part from the periplasmic side of the membrane, the one in the C-terminal domain (region XA) from the cytoplasmic side (trans pore loops). The two re-entrant loops are believed to be in close vicinity in the 3D structure and to form the translocation pathway for co-ions and substrates. The binding site is believed to be positioned at the membrane-cytoplasm interface where an arginine residue interacts directly with the bound substrate. Different families may have additional TMSs at the N- or C-termini or in between the two domains. The transporters of the 2HCT family have one additional TMS at the N-terminus locating the latter in the cytoplasm. The odd number of TMSs in each domain forces the orientation of the two domains in the membrane to be opposite; the N-terminus of the N-terminal and C-terminal domains resides in the periplasm and cytoplasm, respectively. The pore loops contain an

extraordinarily high fraction of residues with small side chains (glycine, serine, and alanine) which may reflect a compact packing of the loops in between the TMSs. The regions containing the pore loops are among the best conserved regions in the transporter families. The two pore loops would be in close contact in the 3D structure in a single pore that alternately would be opened to either side of the membrane during the catalytic cycle.

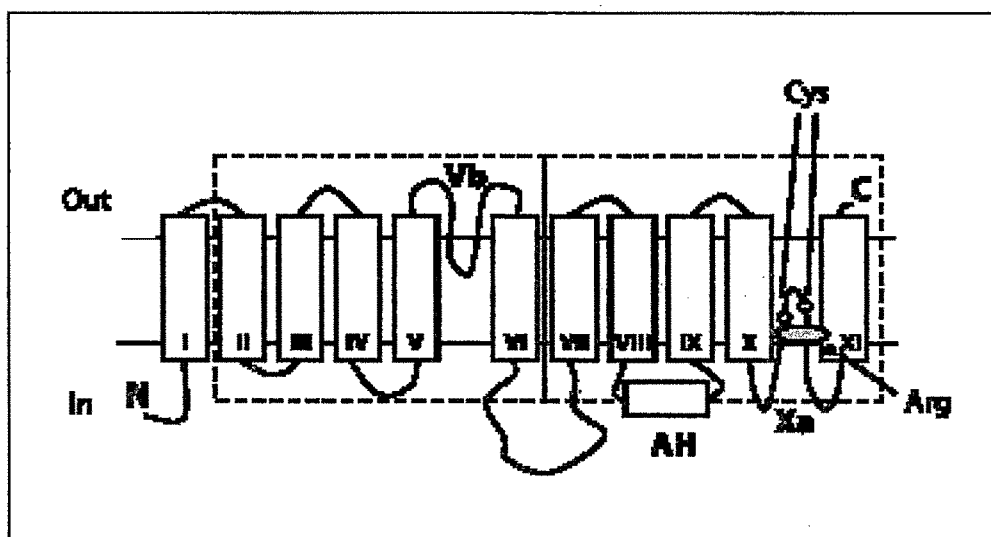


Figure 4.1: Structural model for 2HCT family transporters (Lolkema, 2006).

The substrate-binding site is located at the membrane-cytoplasmic interface, which positions it deep down in the pore when opened to the external face of the membrane. The cytoplasmic pore loop (XA) extends into the pore beyond the binding site, making cysteine residues in the loop accessible from the periplasmic side even when substrate is bound. Opening and closing of the pore to either site of the membrane would be controlled by binding of the substrate and co-ions. The accessibility of cysteine residues in the cytoplasmic pore loop was shown to be different in different catalytic states of the transporter by experiment.

4.1.2 Factors contributing to the low efficiency of the native transporter in fluorescent pseudomonads

Citrate transporter of fluorescent pseudomonads falls under the Major Facilitator Superfamily (MFS) which is a large and diverse group of secondary transporters that includes uniporters, symporters, and antiporters. MFS proteins facilitate the transport of citric acid across cytoplasmic or internal membranes solely by proton driven citrate symport mechanism. Transcriptome analysis of MFS protein have been reported in several pseudomonads viz., *Pseudomonas syringae* Cit7 (359 amino acid, accession AEAJ01000831.1), *Pseudomonas putida* KT2440 (434amino acids, accession AE015451.1, *Pseudomonas aeruginosa* PAO1 (429 amino acids, accession NC_002516.2), *Pseudomonas aeruginosa* PA7 (429amino acids, accession NaC_009656.1).

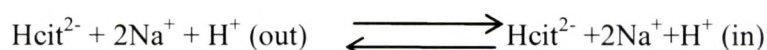
Enhanced accumulation of intracellular citric acid in *P. fluorescens* leads to secretion of citrate by the organism whereas the wild type does not secrete any citric acid to the extracellular medium. But the secretion is not at par with the intracellular accumulation revealing the low efficiency of the citrate transporter (Buch et al., 2009). The low efficiency of the native citrate transporter in *Pseudomonas* sp. can be attributed to lower intracellular proton levels limiting the citrate efflux. *Pseudomonas* sp. being neutrophiles always try to maintain a lower extracellular pH compared to intracellular pH indicating that proton concentration is higher outside (**Table 4.3**). pH homeostasis in these bacteria resist the change in pH across the cell membrane and does not allow overflow of proton across the membrane.

Citric acid secretion could be stabilized if there were a mechanism whereby the cells could secrete elevated levels (Delhaize et al. 2004). Na⁺ dependent citrate transporters are highly specific for citrate. The major species transported across the cell is HCit²⁻. It accumulates citrate at the expense of Na⁺ concentration gradient generated by various sodium ion pumps.

Table 4.3: pH homeostasis in bacteria (White, 2010)

BACTERIA	pH _{out}	pH _{in}	pH _{in} -pH _{out}
Neutrophile	6-8	7.5-8	+
Acidophile	1-4	6.5-7	+
Alkaliphile	9-12	8.4-9	-

Reaction :



Mainly these transporters function in citrate uptake inside the cells. **Fig. 4.2** represents the schematic representations of the pathways-

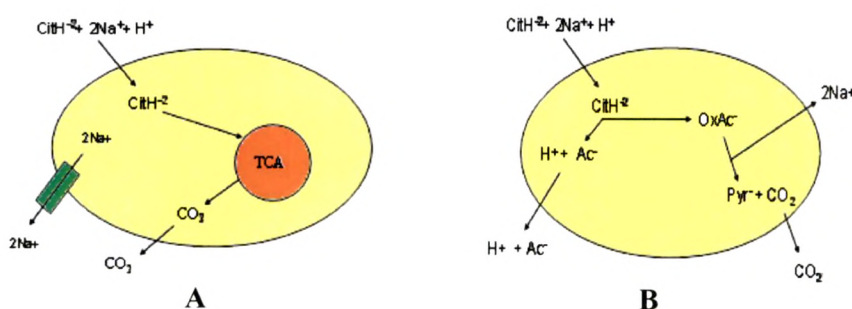


Figure 4.2: Na⁺ efflux mechanisms in bacteria. (A). Aerobic and (B). Anaerobic conditions (Lolkema, 1994).

All bacterial cells although maintain an intracellular Na⁺ concentration lower than the extracellular, intracellular concentration above 20mM is harmful to *E. coli* and in halophiles is above 3M (Lolkema, 1994). Bacterial cells protect from the adverse effects of Na⁺ by primary and secondary Na⁺ extrusion system. NhaA, the Na⁺/H⁺ antiporter is the system responsible for adaptation to Na⁺ and alkaline pH (**Fig. 4.3**). All bacterial cells maintain the optimum intracellular Na⁺ levels by (i) Symport with metabolites and antiport against H⁺ are widely used mechanisms in almost all bacteria for Na⁺ influx and efflux; (ii)

Decarboxylases and ATPases function in anaerobic bacteria. Decarboxylases act as Na^+ pumps for efflux and ATPases use the energy obtained by influx of Na^+ down its concentration gradient for ATP synthesis; (iii) Marine organisms have respiratory chain mechanism for efflux of Na^+ to maintain sodium motive force (smf) and flagella motors which use energy derived from influx of Na^+ down the concentration gradient.

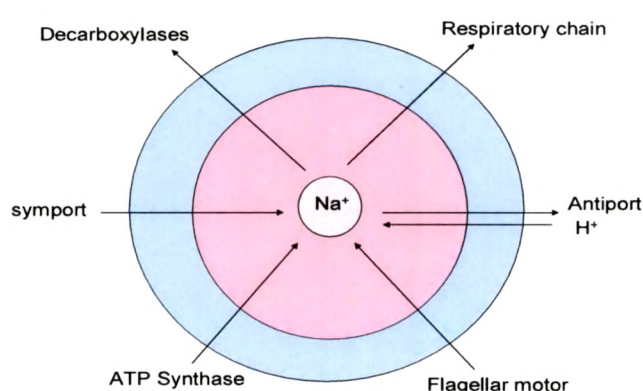


Figure 4.3: Bacterial stress responses and Na^+ homeostasis (Storz et al.,1996)

4.2 Rationale of the present work

Reversibility is recognized as a fundamental feature of coupled vectorial transport systems. Therefore, the decarboxylase systems could also function in reversible manner wherein the direction of operation depends on the cation gradient and free energy change under the conditions of the physiological steady state. Heterologous overexpression of citrate symporter coupled to Na^+ and Mg^{2+} may play an important function as an alternative pump for efflux of Na^+ and/or Mg^{2+} (**Fig.4.2**) along with citrate. The present study demonstrates the effect of heterologous overexpression of *S. typhimurium* Na^+ dependent and *B. subtilis* Mg^{2+} dependent citrate transporter on citric acid secretion by *P. fluorescens* PfO-1.

4.3 WORK PLAN

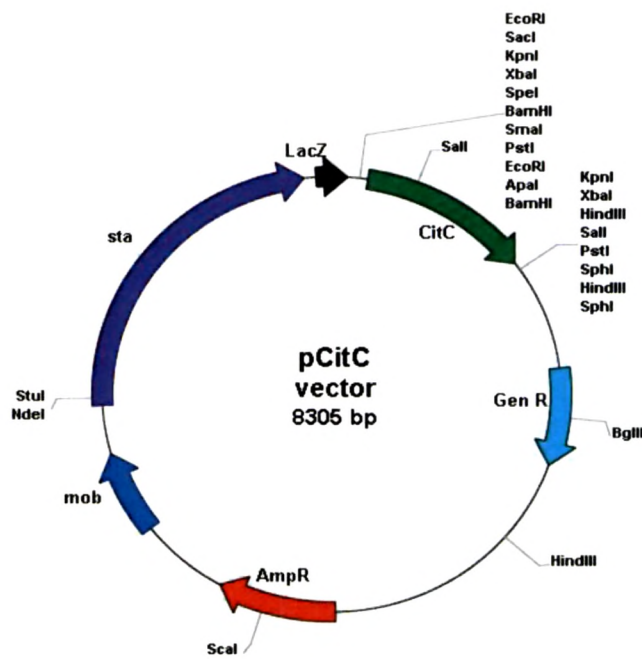
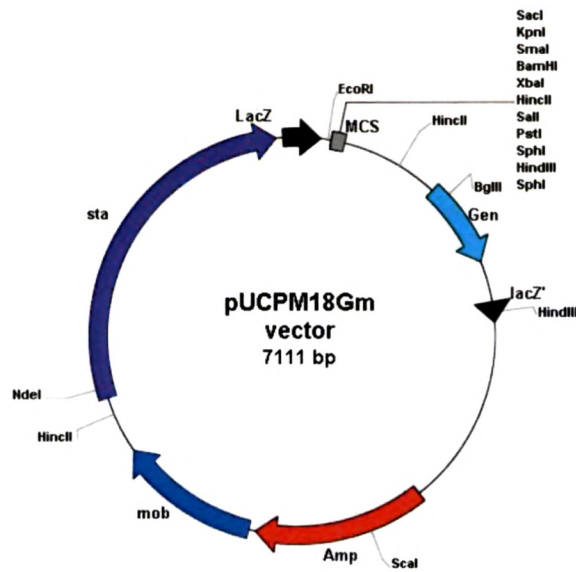
The experimental plan of work includes the following-

4.3.1 Bacterial strains used in the study

Table 4.4: List of bacterial strains used.

Bacterial strains	Characteristics	Source/Reference
<i>E. coli</i> DH5 α	F- ϕ 80 Δ lacZ Δ M15 Δ (lacZYA-argF) U169 <i>recA1 endA1 hsdR17</i> (rk-, mk+) <i>phoA supE44 λ-thi-1 gyrA96 relA1</i>	Sambrook and Russell, 2001
<i>E. coli</i> W620	CGSC 4278 - <i>glnV44 gltA6 galK30</i> <i>LAM-pyrD36 relA1 rpsL129 thi-1</i> ; Str ^r	<i>E. coli</i> Genetic Stock Center
<i>Salmonella typhimurium</i>	Sewage isolate	Kumar, 2012
<i>Bacillus subtilis</i> 168	Wild type strain	ATCC
<i>P. fluorescens</i> Pfo-1	Wild type strain	
<i>Pf</i> (pGm)	<i>P. fluorescens</i> Pfo-1 with pUCPM18; Gm ^r	This Chapter
<i>Pf</i> (pCitC)	<i>P. fluorescens</i> Pfo-1 with pCitC; Gm ^r	This Chapter
<i>Pf</i> (pCitM)	<i>P. fluorescens</i> Pfo-1 with pCitM; Gm ^r	This Chapter
<i>Pf</i> (pYFpCitC)	<i>P. fluorescens</i> Pfo-1 with pY146F and pCitC double transformant ; Km ^r , Gm ^r	This Chapter
<i>Pf</i> (pYC)	<i>P. fluorescens</i> Pfo-1 with pYC; Gm ^r	This Chapter

Detailed characteristics of these strains and plasmids are given in Section 2.1. Parent strains and the transformants of *E. coli* and *Pseudomonas* were respectively grown at 37°C and 30°C with streptomycin, kanamycin and gentamycin as and when required, at final concentrations varying for rich and minimal media as described in Section 2.2, Table 2.4.



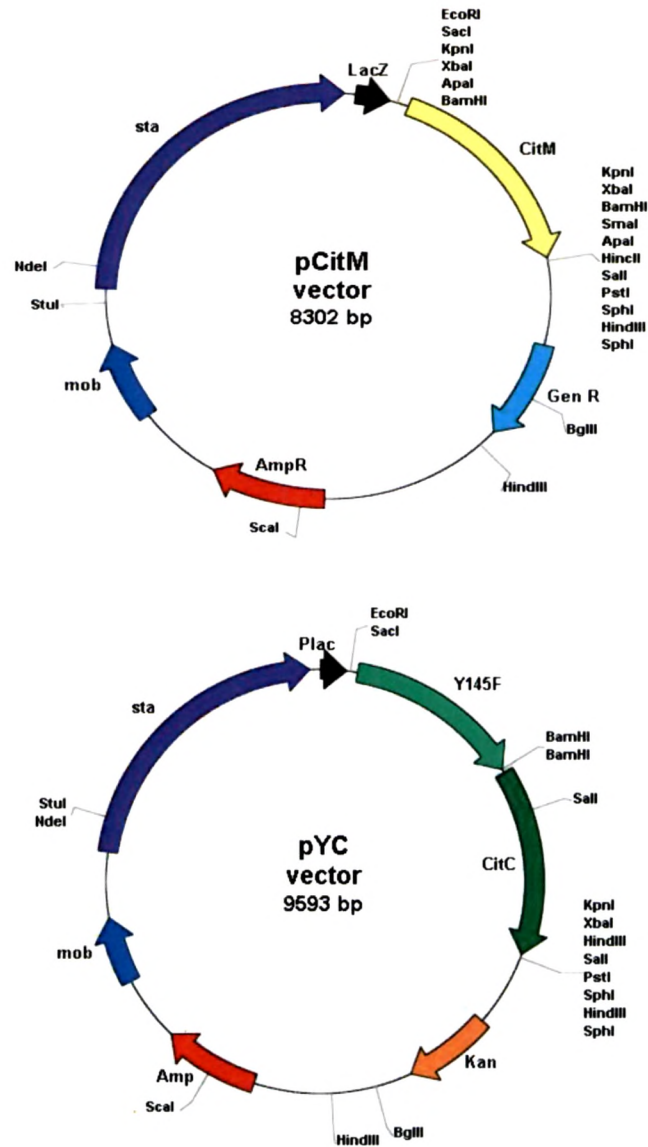


Figure 4.4: Restriction enzyme map of broad host range pUCPM18 vector having gentamycin resistance.

(a) pUCPM18Gm vector, (b) pUCPM18 vector containing *citC* gene in XbaI site,(c) pUCPM18 vector containing *citM* gene in EcoRI-SalI site, (d) pUCPM18Gm vector containing NADH insensitive *cs* Y145F gene and *citC* gene under the same *lac* promoter.

4.3.2 Construction of *Pseudomonas* stable plasmid containing *S. typhimurium* Na⁺ citrate transporter (*citC*) and *B. subtilis* Mg²⁺ citrate transporter (*citM*) genes under *lac* promoter

The strategy for construction of pCitC and pCitM plasmid and their transformation in *P. fluorescens* Pfo-1 strain harbouring NADH insensitive *cs* gene are depicted in Fig.4.5-4.6.

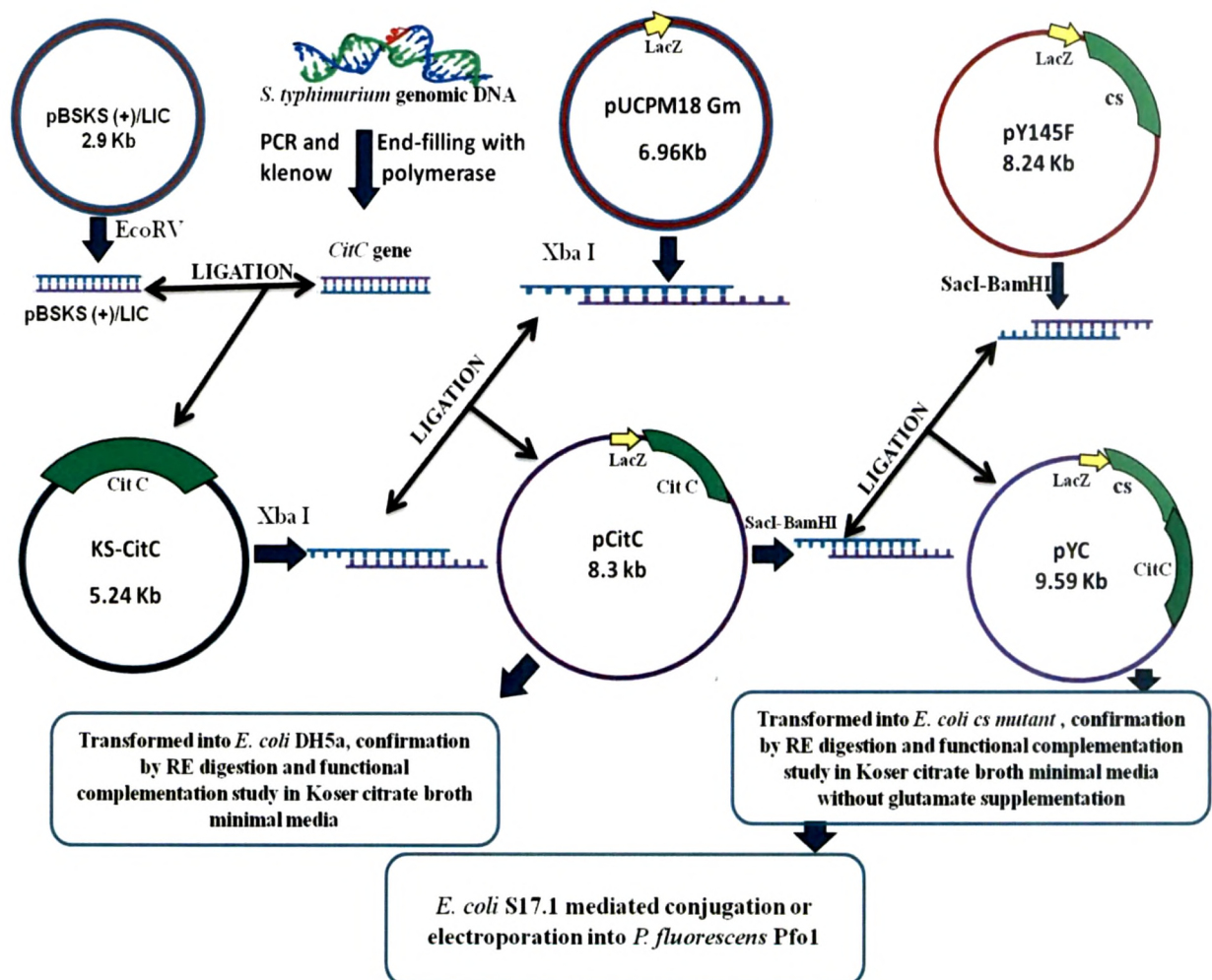


Figure 4.5: Strategy for cloning of *Salmonella typhimurium* citrate transporter (*citC*) gene and YC operon in broad host range vector pUCPM18 having gentamycin resistance.

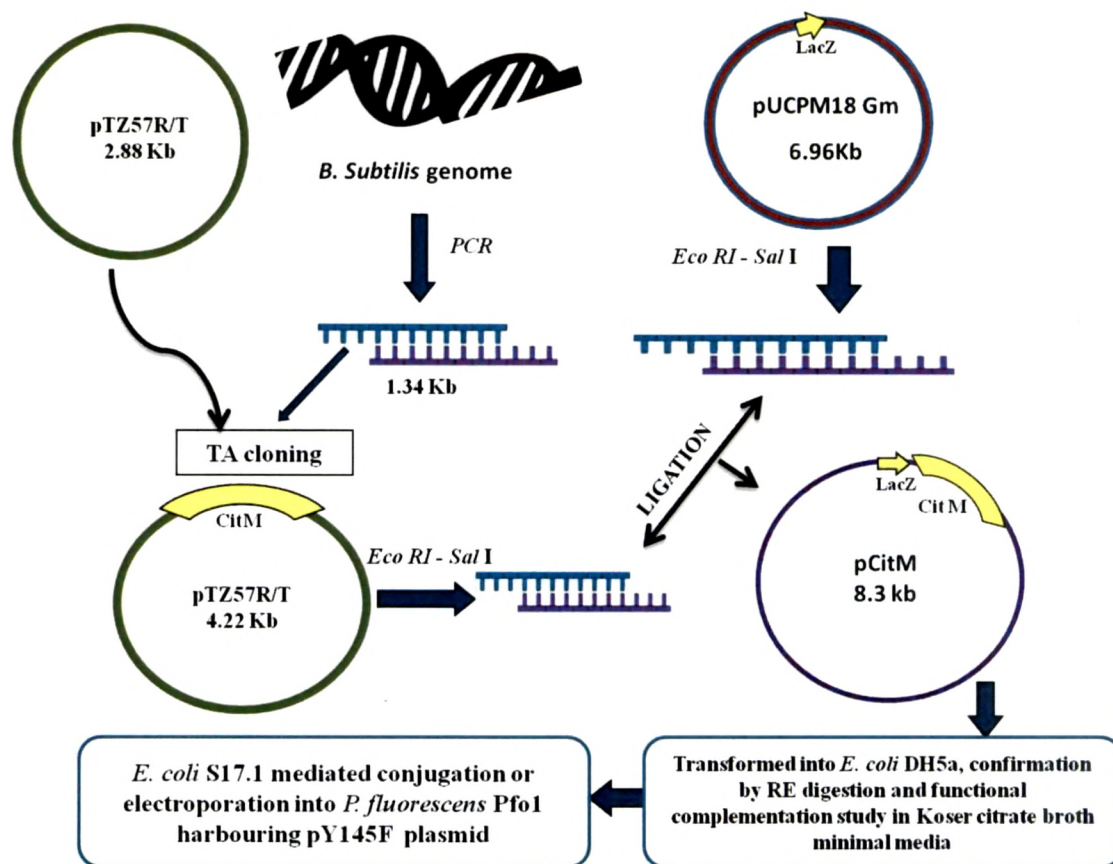


Figure 4.6: Strategy for cloning of *Bacillus subtilis* citrate transporter (*CitM*) gene in broad host range vector pUCPM18 having gentamycin resistance.

Gene specific primers are designed using *citC* gene sequence from *Salmonella typhimurium* LT2 strain (ATCC 700720, Gene Bank accession number: EMBL P0A2F8) and *citM* gene sequence from *B. subtilis* 168 strain (Gene Bank accession number: U62003) (Table 4.5). Cloning of isolated *citC* gene was carried out in pBluescript vector using *Sma*I site and confirmed by double digestion with *Eco*RI-*Sal*I and *Eco*RI-*Bam*HI restriction site (Fig. 4.5). Subcloning of *citC* gene was carried out in pUCPM18 Gm vector having gentamycin resistance and the recombinant plasmid was confirmed by restriction mapping. In the other strategy the isolated *citM* gene was first cloned into pTRZ57/R

followed by cloning into broad host range vector pUCPM18Gm using EcoRI-SalI restriction site. All constructs were confirmed by restriction enzyme digestion and PCR.

Table 4.5: List of primers. *Pseudomonas* sp. specific RBS highlighted in yellow is added in each primer before the start side

Primer	Sequence (5'-3')	Tm/GC%
Na⁺ dependent citrate transporter		
FNa ⁺ Apal BamHI:	GGGGGCCCCGGGATCCCG CACGGAGGAATCAACTTATG ACC AAC ATG ACC CAG GCT TC	59.6°C, 52.2%
RNa ⁺ KpnI XbaI	GGGGTACCCCGCTCTAGAGC TTA CAC CAT CAT GCT GAA CAC GAT GC	59.6°C, 46.2%
Mg²⁺ dependent citrate transporter		
F Apal BamHI	GGGGGCCCCGGGATCCCGCACGGAGGAATCAACTT ATG TTA GCA ATC TTA GGC TTT CTC ATG ATG	57.7°C, 40%
R KpnI XbaI	GGGGTACCCCGCTCTAGAGC TTA TAC GGA AAT AGA GAT CGC ACC G	58.2°C 48%

Apal BamHI: GGGGGCCCCGGGATCCCG KpnI XbaI: GGGGTACCCCGCTCTAGAGC

RBS: 5' CACGGAGGAATCAACTT 3'

4.3.3 Functional confirmation of *CitC* and *CitM* gene expressed from pCitC and pCitM plasmids.

E. coli DH5 α being a mutant of citrate transporter was used to determine the functionality of the transporter gene. *E. coli* DH5 α containing pCitC and pCitM along with the respective controls pGm plasmid subjected to growth on Koser citrate broth containing citric acid as a sole carbon source supplemented with 100mg/ml thymine and 0.1mM IPTG.

4.3.4 Development of *P. fluorescens* PfO-1 harboring pYF-pCitC and pYF-pCitM plasmid.

The recombinant plasmids pCitC and pCitM were transformed by electroporation in *P. fluorescens* PfO-1 harbouring NADH insensitive cs plasmid pY145F . The double transformants were selected on pseudomonas agar plate containing both kanamycin and gentamycin. *P. fluorescens* PfO-1 containing pAB8 and pGm dual plasmids were used as

control in the experiments. All transformants were confirmed by fluorescence and restriction enzyme digestion of the isolated plasmids from the respective strains

4.3.5 Effect of transporter gene expression on the citric acid secretion and overall physiology and glucose metabolism of *P. fluorescens* PFO-1.

P. fluorescens PFO-1 transformants were subjected to physiological experiments involving growth and organic acid production profiles on M9 minimal medium with 100mM glucose as carbon source. The samples withdrawn at regular interval were analyzed for O.D.600nm, pH, and extracellular glucose. Stationary phase cultures harvested at the time of pH drop were subjected to organic acid estimation using HPLC (Section 2.7.3). The physiological parameters were calculated as in section. The effectiveness of the transporters were compared based on the improvement of citric acid secretion ability. The enzyme assays were performed as described in Section, with CS, G-6-PDH, ICDH PYC being assayed in both mid-log to late-log and stationary phase cultures while ICL and GDH are being assayed in the mid log and stationary phase cultures, respectively.

4.3.6 Construction of *Pseudomonas* stable plasmid containing *cs* Y145F and *citC/citM* genes under *lac* promoter as operon.

The recombinant construction, functional and biochemical characterization of pYC is constructed in similar way as depicted in section..

4.4 RESULTS

4.4.1 Cloning of *S. typhimurium* Na⁺ citrate transporter (*citC*) and *B. subtilis* Mg²⁺ citrate transporter (*citM*) gene:

Gradient PCR amplification of genomic DNA isolated from *Salmonella typhimurium* sewage isolate and *B. subtilis* 168 strains was carried out using gene specific primer to get an amplicon of 1341 bp *citC* gene (Fig. 4.7-4.8). The PCR product was also confirmed by restriction enzyme mapping (Fig. 4.9). The plasmids pCitC and pCitM containing *S. typhimurium* sodium citrate transporter (*citC*) and *B. subtilis* magnesium citrate transporter

(*CitM*) gene, respectively, under *lac* promoter of pUCPM18 plasmid with *Gm^r* gene were constructed as schematically represented and discussed in section 4.3.2. All plasmids were confirmed based on restriction digestion pattern (Fig. 4.10-4.13)) and PCR (Fig. 4.14).

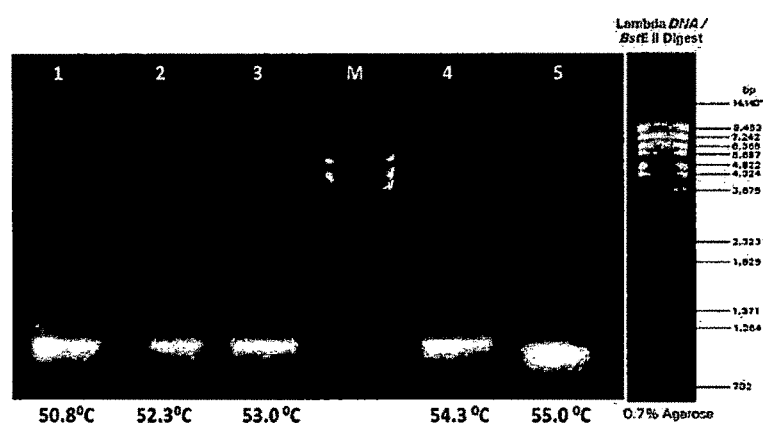


Figure 4.7: PCR amplification of *CitC* gene from *S. phimurium* genome. Lane1-5: *citC* gene at different annealing temperature mentioned in the subsequent lane (1342bp). LaneM: MWM lambda DNA BstEII digest.

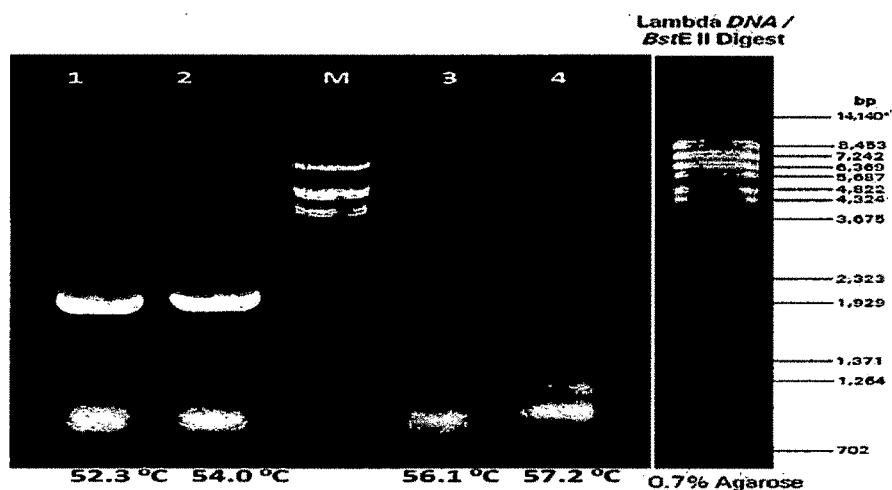


Figure 4.8: PCR amplification of *CitM* gene from *B. subtilis* genome. Lane1-4: *citM* gene at different annealing temperature mentioned in the subsequent lane (1341bp); laneM: MWM lambda DNA BstEII digest.

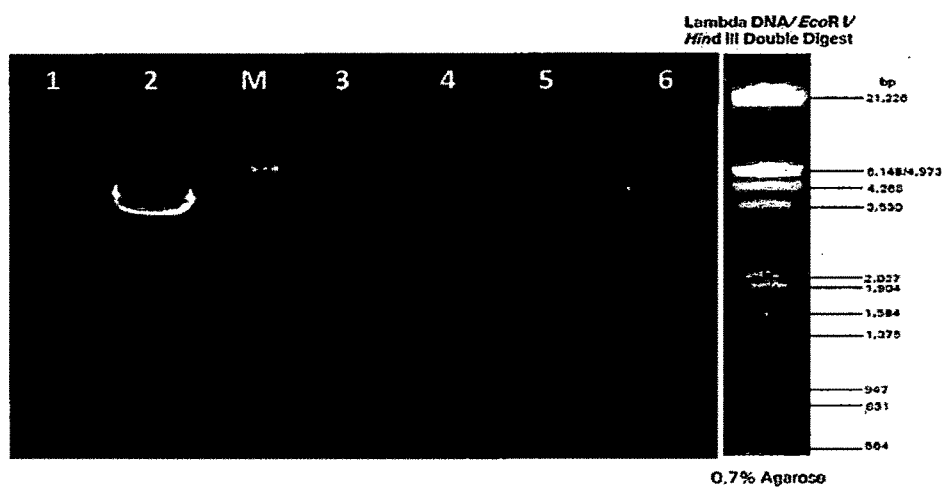


Figure 4.9: Restriction enzyme mapping of *citC* and *citM* gene. Lane1: *CitC* PCR product digested with *SalI* (0.733Kb, 0.51Kb), Lane2: undigested pUCPM18Gm plasmid; Lane3: *CitM* PCR product digested with *XhoI* (0.814Kb, 0.488Kb), Lane4: *CitM* PCR product digested with *HindIII* (0.688Kb, 0.614Kb); Lane5: *CitC* PCR product (1.34Kb); Lane6: pUCPM18Gm plasmid digested with *BamHI* (6.97Kb)

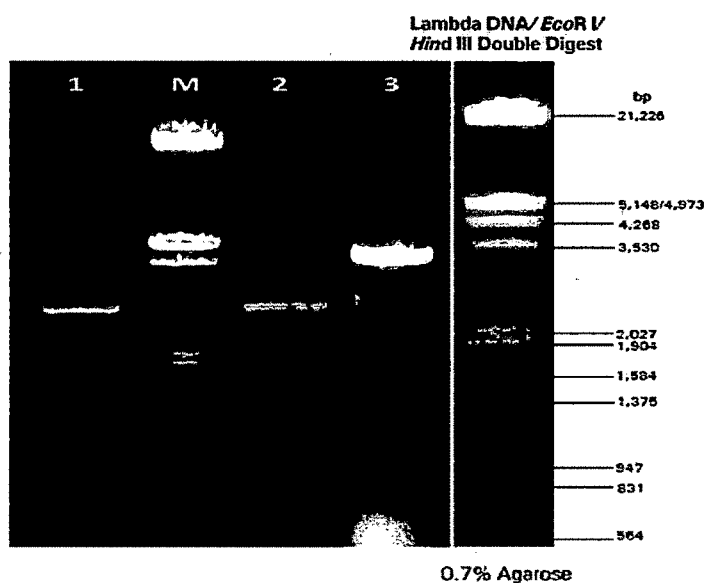


Figure 4.10: Restriction enzyme digestion pattern for pBluescript KS *CitC* clone. Lane1: pBluescript *CitC* plasmid digested with *EcoRI-SalI* (2.9 Kb, 0.8 Kb, and 0.5 Kb); Lane 2: pBluescript *CitC* plasmid digested with *EcoRI-BamHI* (2.9Kb,1.341Kb), Lane3: undigested pBluescriptKS plasmid; LaneM:MWM lambda DNA cut with *EcoRI-HindIII*

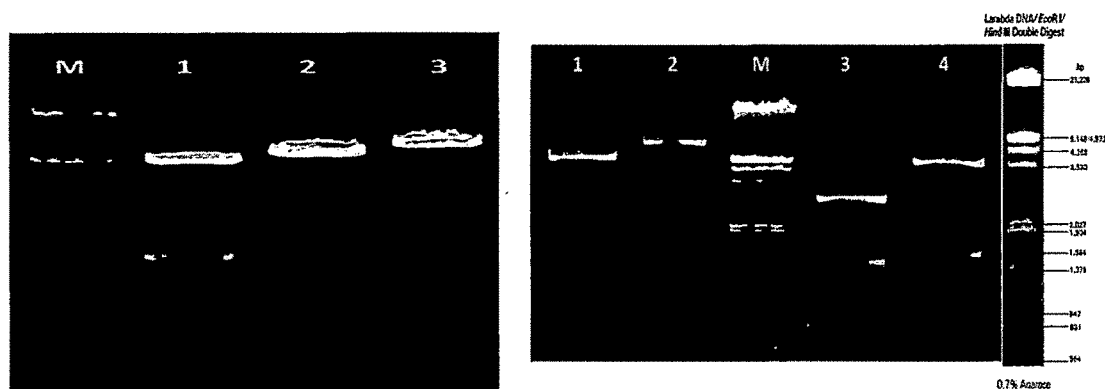


Figure 4.11: Restriction enzyme digestion pattern of pUCPM18Gm vector. Lane1:pUCPM18Gm digested with HindIII(5.3Kb,1.6Kb); lane2: pUCPM18Gm digested with EcoRI-BglII (6Kb,0.9Kb); pUCPM18Gm digested with EcoRI (6.9Kb).

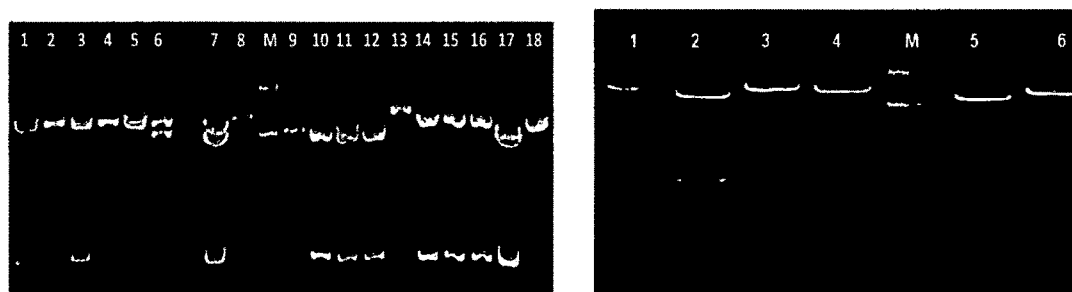


Figure 4.12: Restriction enzyme digestion pattern of pUCPM18Gm CitC vector. (a) Lane1-18: pCitC plasmid digested with BamHI, Lane 13 showing the right orientation clone (8.3Kb). (b) Lane1: pCitC plasmid digested with EcoRI ; Lane2: pCitC plasmid digested with HindIII; Lane3: pCitC plasmid digested with BamHI; Lane4: pCitC plasmid digested with KpnI; Lane5: pCitC plasmid digested with EcoRI-SalI (6.9Kb, 0.81Kb, 0.488 Kb) ; Lane6: pCitC plasmid digested with ScaI (8.3Kb)

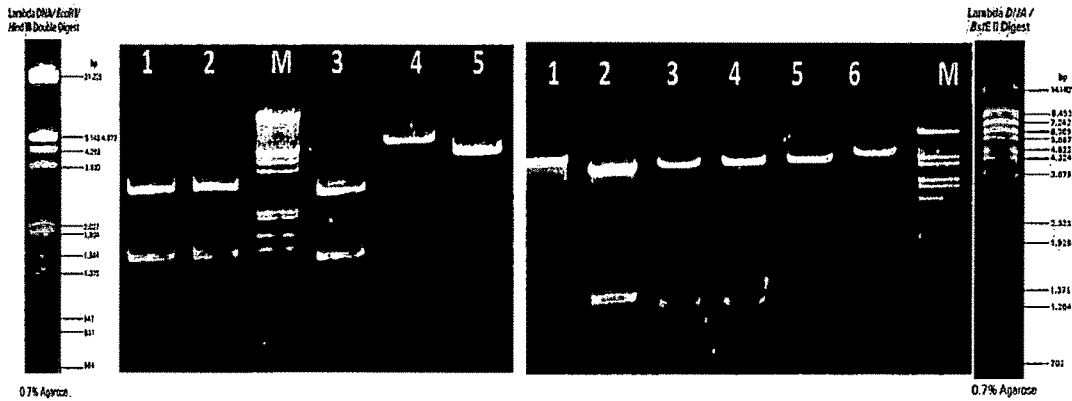


Figure 4.13: Restriction enzyme digestion pattern of pCitM clone. (a) Lane1: pTRZ57/R CitM digested with BamHI (2.88Kb,1.34Kb); Lane2: pTRZ57/R CitM digested with EcoRI-Sall (2.88Kb,1.34Kb); Lane3: : pTRZ57/R CitM digested with KpnI; Lane4:pUCPM18Gm vector digested with EcoRI-Sall (6.9Kb); Lane5: pUCPM18Amp vctor digested with EcoRI-Sall; LaneM: MWM lambda DNA EcoRI-HindIII double digest. (b) Lane1:pCitC plasmid digested with bamHI (8.3Kb); lane2:pCitC plasmid digested with XbaI (6.9Kb,1.34 Kb); Lane3:pCitM plasmid digested with BamHI (6.9Kb,1.34Kb); Lane4:pCitM plasmid digested with XbaI (6.9Kb,1.34Kb); Lane5:pCitM plasmid digested with KpnI (6.9Kb,1.34Kb); lane6::pCitM plasmid digested with ApaI (8.3 Kb); LaneM: MWM lambda DNA BstEII digest.

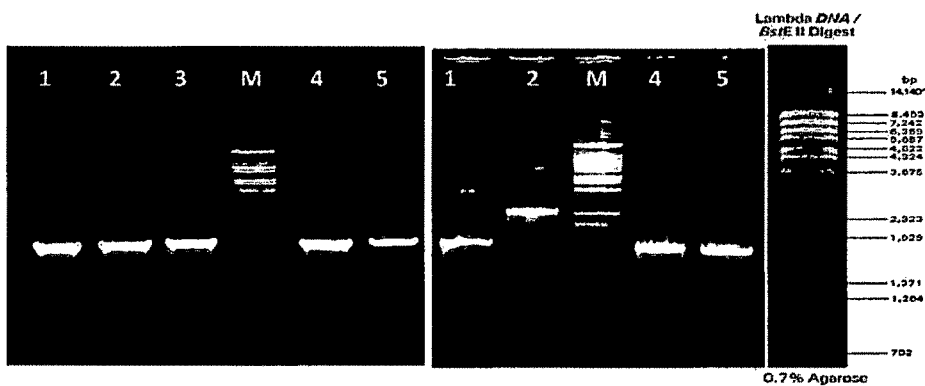


Figure 4.14: PCR amplification of *citC* and *citM* transporter gene cloned in pUCPM18 Gm^r vector.(a) Lane1-2: pUCPM18Gm vector containing *citC* gene ; Lane3-5: pUCPM18Gm vector containing *CitM* gene amplified using gene specific primer.. (b) Lane1: pUCPM18Gm vector containing *citC* gene amplified using *plac* forward and *CitC* reverse primer; Lane2: pUCPM18Gm vector containing *citM* gene amplified using *plac* forward and *CitM* reverse primer; Lane 3-4: pUCPM18Gm containing *citC* and *citM* gene, respectively amplified by using gene specific primer.

4.4.2 Construction of *Pseudomonas* stable vector containing NADH insensitive *cs* gene Y145F and *S. typhimurium citC* gene under *lac* promoter of pUCPM18 Gm^r plasmid:

The plasmid pYC containing NADH insensitive *cs* gene Y145F and *S. typhimurium citC* gene under *lac* promoter of pUCPM18 Gm^r plasmid were constructed as schematically represented (Fig. 4.5). The plasmids were confirmed by restriction enzyme digestion and PCR (Fig. 4.15)

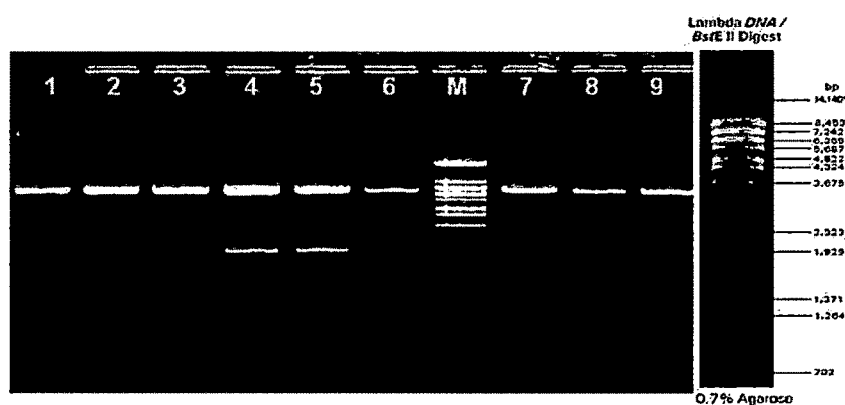


Figure 4.15: Restriction enzyme digestion pattern of pYC plasmid containing NADH insensitive Y145F gene and *S. typhimurium* sodium citrate transporter gene under same *lac* promoter in pUCPM18 Gm. Lane1-9: pYC plasmid digested with EcoRI-XbaI (6.97 Kb,2.62Kb), LaneM: MWM lambda DNA BstEII digest.

4.4.3 Confirmation by sequencing

4.4.3.1 16s rRNA gene partial sequence of *Salmonella* sp. WT

Analysis of the 16s sequence data of *Salmonella* sp. sewage isolate using NCBI blast online homology programme revealed maximum identity (99%) to *Salmonella*. The GenBank accession number obtained for this partial 16S rDNA sequence is JN555586 and the accession profile is given in Fig.4.16.

```

LOCUS       JN555586                887 bp    DNA     linear   BCT 06-SEP-2011
DEFINITION  Salmonella sp. WT 16S ribosomal RNA gene, partial sequence.
ACCESSION   JN555586
VERSION     JN555586.1   GI:345286192
KEYWORDS    .
SOURCE      Salmonella sp. WT
  ORGANISM  Salmonella sp. WT
            Bacteria; Proteobacteria; Gammaproteobacteria; Enterobacteriales;
            Enterobacteriaceae; Salmonella.
REFERENCE   1 (bases 1 to 887)
  AUTHORS   Kumar,P., Adhikary,H., Kumar G,N. and G,A.
  TITLE     A metabolic study of engineered fluorescence Pseudomonads strains
            for high citric acid secretion
  JOURNAL   Unpublished
REFERENCE   2 (bases 1 to 887)
  AUTHORS   Kumar,P., Adhikary,H., Kumar G,N. and G,A.
  TITLE     Direct Submission
  JOURNAL   Submitted (30-JUL-2011) Biochemistry, M S University of Baroda,
            Faculty of Science, Vadodara, Gujarat 390002, India
COMMENT     Sequences were screened for chimeras by the submitter using
            Ribosomal Database Project (RDP) II.
FEATURES             Location/Qualifiers
     source           1..887
                     /organism="Salmonella sp. WT"
                     /mol_type="genomic DNA"
                     /strain="WT"
                     /isolation_source="unprocessed sewage"
                     /db_xref="taxon:1077200"
                     /country="India: Vadodara, Gujarat"
                     /lat_lon="22.30 N 73.20 E"
     rRNA             <1..>887
                     /product="16S ribosomal RNA"

```

Salmonella sp. WT 16S ribosomal RNA gene, partial sequence

GenBank: JN555586.1

[GenBank](#) [Graphics](#)

>gi|345286192|gb|JN555586.1| Salmonella sp. WT 16S ribosomal RNA gene, partial sequence

```

CGTCGCACGACAAAGAGGGGCGACTTCCGCGCTCTCTCCATCAGATCGCGCGAGATGTGATCAGCTAGT
TGCTGAGGTACCGCTCACCAGGGCGACGNTCCCTAGCTGGTCTGAGAGGATGACCAGCCACACGGGAAT
TGAGACACGGTCCAGACTCATA CGGGAGGCAGCAGTGGGGAATATTGCACAAATGGCGCACGCTTGATGC
AGCCATGCCGCTGTATGAAGAAGGCTTTCGGGTTGTAAAGTACTTTTAGCGGGGAGGAAGGTGTGTGG
TTNATAACCCGACGCAATIGACGTTACCCGACAGAAGCACC GGCTAACTCCGTGCCAGCAGCCCGGTA
ATACGGAGGGTGCRAAGCGTTAATTGGAATTACTGGGCGTAAAGCGCACGCAGGCGGCTCTGTCAAGTAGGA
TGTGAAATCCCGGGCTCAACCTGGGAACIGCATTGAAACTGGCAGGCGCTGAGTCTCTAGAGGGGGGTA
GAATCCAGGTGTAGCGGTGAARTGCGTAGAGATCTGGAGGAATACCGGTGGCGRAGGCGGCCCCCTGGA
CAAGACTEACGCTCAGGTGCGAAGCGTGGGAGCAACAGGATTAGATACCCTGGTAGTCCACGCCCT
AACGATGTCTACTTGGAGGTTGTGCCCTGAGGCGTGGCTTCCGGAGCTAACCCGTTAAGTAGACCCCT
GGGAGTACGGCCGCAAGGTTAAAACCTCRAATGAATTGACGGGGCCGCACAGCGGTGGAGCATGTGG
TTTAAATTCGATGCARCCGGAAGAACCTTACCTGGTCTTGACATCCACAGAACTTCCAGAGATGGAAGG
TGCTTTCGGGAACCGTGCAGACAGGTGCTGCATGGCTGTCTGCCAGCC

```

Figure 4.16: GenBank accession result of partial 16S rDNA sequence of *Salmonella* sp. WT

4.4.3.2 Partial SPA sequencing of *citC* and *citM* gene

NCBI-BLAST analysis of the SPA sequencing results done by using both forward and reverse primer revealed maximum homology of the *citC* gene to *S. enteric sp. enteric serover* Heidelberg Na⁺ citrate (OH) antiporter and *S. enteric sp. enteric serover* Gallinarum citrate sodium symporter (98%) and of the *citM* gene to *B. subtilis* subsp. *subtilis* str. 168 transporter of divalent metal ion /citrate complexes and *B. subtilis citM* gene (96%).

```

>YFCitc_CitcFor_s665
NNGNGGGCGGACGGAGAAAAAGGGGGCTAGCGATTACTCAGATTCAAAATCTTTGGTAT
GCCGCTACCGCTTTATGCCTTTGCATTAATTACTTTATTACTTTCTCATTTTTATAATGC
TATACCGACTGACTTAGTCGGTGGTTTTGCCCTTATGTTTGTGATGGGGCCATTTTTGG
TGAAATCGGCAAACGTTTACCGATCTTCAATAAATATATTGGCGGGCCACC GGTTATGAT
ATTTCTGGTTGCAGCTTATTTTGTCTATGCTGGCATATTTACGCAAAAAGAAATTGATGC
GATCAGCAACGTAATGGATAAAAGCAACTTCCTTAACCTGTTTATCGCAGTGTGATCAC
AGGCGCGATCCTGTGCGTAAACCGTAAGCTGCTATTAATAACTACTGCTGGGCTATATCCC
AACCATCCTCGCCGGATTTGTCGGCGCGTCCCTTTTCGGTATCGTCATTGGTCTGTGCTT
CGGTATCCCGGTCGACCGTATCATGATGCTGTACGTTCTGCCGATTATGGGCGGTGGTAA
CGGCGCGGGCGCCGTGCTCTGTCTGAAATTTATCACTCGGTTACCGGACGTTCTCGCGA
AAAGTATTACTCAACGGCTATTGCTATTCTGACCATGCGAATATCTTCGCCATTATTTT
CGCCGCCCTCCTCGATATGATAGGCAAAAAATACACCTGGCTTAGCGGTGAAGGTGAGTT
GGTTGTAAGGCTTCCTTCAAACCGAAGATGATGAAAAGGCCGGTCAGATTACCCATCG
TGAAACGGCGGTTGGCATGGTGTATCCACCACCTGCTTCCTGCTGGCCTATGTTGTTGC
AAGAAAATTTCTGCCAGCATCGGCGGGCTCTCTATTCACTACTTCGCCCTGGATGGTCTG
ATTGTTGCTGCGCTGAACGCATCAGGCTTTTGTCAACGGAGATTAAGCCGGGGCGAANT
CTTTCTGACTTCTTCTCAAACAGCTGCTGGGGNATGGA

>YFCitc_CitcRev_s665
NNCNTTTGTAGCCCGATAAACCAGCACAATACCGCCGCCAGACGAGAGGAAATTTGTGC
ATATGAANTGAGGTTACATACGGTTACAGGCGGAGAGCACTTCCAGATCGCCGGAGCCGCC
CGGTTGGCCATACAAAGACCCGCGAGTAATGGATGATTCAATCGGGTAGAAGCCAATCAA
CCAGCCCCCGATAGCTGCGCCGACGACTGCGCCGACCACGATGATCGCGGCATAACGAC
GTTGCGGAACGTCAGGCATCGATGATCTCTTGCAGATCGGTGTAGCAAACACCCACACC
TACCATCAATACCCACAGCAGCTGTTTGGAGAAGAAGTCAGAAAGACGTTTCGCCCCGGC
TTTAATCTCCGGTGAGCAAAGGCCTGATGCGPTTCAGCGCAGCAACAATCAGAACCATCCA
GGCGAAGTAGTGAATAGAGACGCCGCGGATGCTTGGCAGAATTTTCTTGGCAACAACATA
GGCCAGCAGGAAGCAGTGGTGGATAGCACCATGCCAACCAGCGTTTCAGGATGGGTAAATC
TGACCGGCCTTTCATCATCTCGGTTTGAAGGAAGCCTTACGAACCAACTCACTTCACTGC
TAGTCAGTGTATTTTTGCCTATCANATCGAGGAGGCGCNAANNATGNGAANNATCGCAT
GTCAGAATAGCATNCCGTNAGTAATACTNTCGCGAGAAGCTCNGTAACCGAGTGGATAA
AGTTGCNNACGNGGCCGGNCCNNNCNTNCAGCCNATCGNNAACGTACGNCTCTTGAT
ACGTCGACCGNNCAGCCAANCATGACCATCGNNNACNCGAATCNGNGGATGNTGAATN
NNNNANGATTTATACCGCTACGGTTACCGCACGATCCGCCNNNNNANNGGANACGGTAA
GNNNNCTTACNNCGTGTGCTGNNCGCCANGNCCGNNATNCGCANAGACAAATN

```

Figure 4.17: Partial SPA sequence of *Salmonella sp. citC* gene


```

>PCITM_citMFor_S701
CCGGGGN GGGNGTGTN NCGAGGCCN NHNTTTTTT GTTTCNTTTN NCTATNNNNNNN
NNNNNAATGGCAATTGAATCATGAACAAAACGGGCTTTCAGTATTAACCAGCCATTAGT
TTTTGACGCCCGAAATTGGTGTTCGGCTCCTTAATCCGCCCGGGAATTTTGGGAATTTT
ACCTGGAAAGTTGGGGGGGAA CAATGGAATGGAATTTTTCGGGGGGGAATTTCCAGCCA
ANGTTCGCGCCCGAAANGGGGGGGTCAATGAATTTAATTGTTTTT GCCCAAATTCCTT
AATATTTTTTTTGGGGAAATTTTATTGAAATTGGAAAAACCCGGGGCCCGGGTTTTTGAA
ATCCCCAAAGGGGGTGGGGGAAAAAATTTTTTAAAACCGGGGNCNAAAAGGGGA
AAAACCCCTTTTAAAAAAAATTTTTTTTTTTTCCGGGGGAAACAACCCGGGTTTTTT
TTTAAAAAAGGCCCC CCCCCCCCCCTTTGAAAAAAGAAAAAAGGGGNCCCCC
CCCCACCCCTTTAAATGGGGTTTTTCCAAAAAAGGGGCCCCCCAGGGGTTTTTTCC
CCCCCCTTTTTTTTTTTGNCCNGNAAGAGGGGNACCCCCCGGGCCAAAATTTTTTTT
TTTTTTTGGGNGAAAGGAAAAACCC CCGGGAGAAACCC CCGGGGGGAAAA
AATTTCTNGAAAAAACTTTTTTTTTTTTTTTTTGGGGGGGAANTGGNGCCCCCCCC
CCCCAAAAGGGGGGGGGGAAAAAAAAC CCCCCCGGGGGGGGGGGTGTTTTTTT
TTCCCCCCCCCGGGGGGAATTTTTTAAAGGCGCCCAACAAAAAAAATACT
CCCCCCCCCTCNTTCTTAAAAAAAAGGGGGGGGGAGGAGGGCGCT

>PCITM_citMRev_S701
NTTNAATCAGAGCGATAGCCGT CATGACGATCACTGCGAGAACCGCCCATTTCAATGCNA
NTTTTTGATGGT CATCAATAGAACTCCGACGAGTCCGACAAGCAAATGAGTGGATGGCA
CAAGCGGACTCAGCATATGAATCGGCTGGCCGATAATAGAGGCTCTGGCAATTTCCACTT
TATCCACACCGTATGCGACAGCTGTTTCTGATAAAATCGGCAGCACC CCGTAGAAATACG
CGTCATTGCGCATCAAAAATGTGAAAATGCCGCTTGTTAAGGCAACAATCGCCGGGATCA
ATCCGCCCATTTGTTCCGGTATCATGGACAGGAGGATCGCCATTTT CATCAACCATTT
TCGTGCCTGTCAAATCCCCGTGAAACCCCCGCGAGCAAAAATCATTGAACCGATGCCA
GCACGTTGTGGAAATGCCGCCGATGCCTGTCTCTGAGCTCAAAANN GGGAAAATTHACN
ATTCAGCGCAATANAAAACGNNNNACNANCAGTCCGGTNAACCTAATTTTCCCNNAACAA
ACTCHNNNTTAAANAANNCGTNANAATANTTNANCNNNANGNTNNNCGTTTCANTATTTNAA
NNNGGNCNNNTTGCTTGNTGGTGTTCATTANCNCCAANGGTTTTCNTNNTNNNNANCAA
ANAATGCACNTAAGNCCGTNNAAGAA GAACTCGGCTNGANCGNNGATANCNAGGGATNN
CNCTGGGNGNNNCTNNGANNNTNCGGGTNCANNANCNNNGATCGGAAAANN

```

Figure 4.19: Partial SPA sequence of *B. subtilis* 168 strain *citM* gene

4.4.4 Functional complementation of pCitC, pCitM and pYC plasmids in *E. coli*.

E. coli DH5 α containing pCitC, pCitM and pYC plasmid grow on Koser citrate broth medium induced with 0.1mM and 0.2 mM IPTG and supplemented with 100 mg/ml thiamine whereas *E. coli* DH5 α containing pGm plasmid failed to grow (Fig. 4.21).

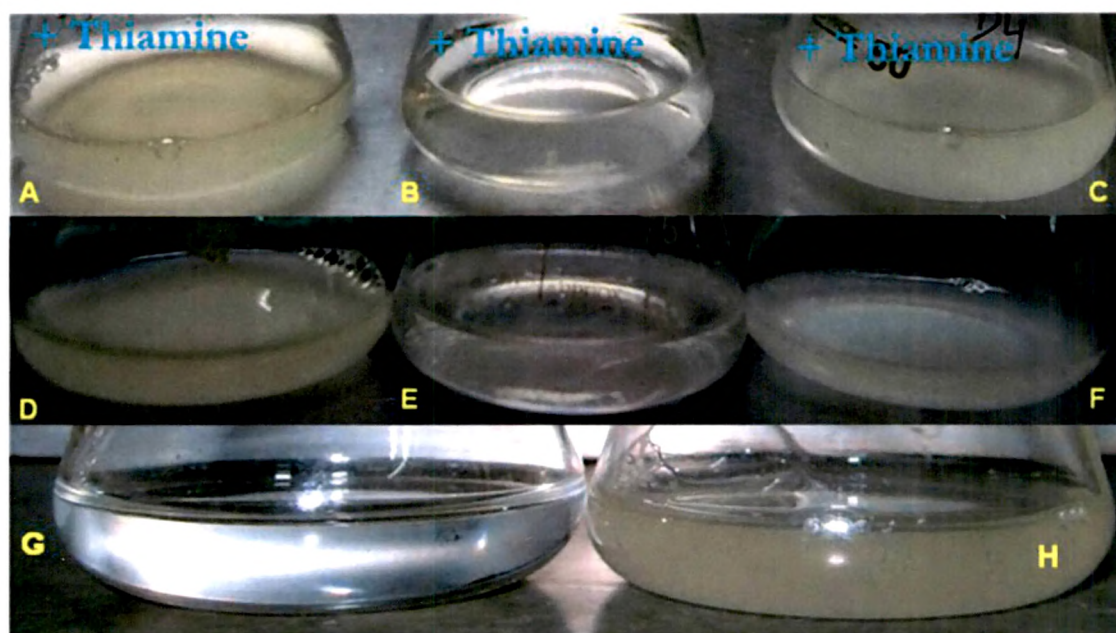


Figure 4.21: Growth of *E. coli* DH5 α on Koser citrate broth. *E. coli* DH5 α containing: pCitC plasmid induced with 0.1mM IPTG (A), pGm plasmid induced with 0.1mM IPTG (B), pCitC plasmid induced with 0.2mM IPTG (C), pCitM plasmid induced with 0.1mM IPTG (D), pGm plasmid induced with 0.1mM IPTG (E), pCitM plasmid induced with 0.2mM IPTG (F), pGm plasmid induced with 0.1mM IPTG (G), pYC plasmid induced with 0.1mM IPTG (H). All plasmid bearing strains are supplemented with 100mg/ml thiamine and antibiotic 1/4th of the recommended dose.

4.4.5 Effect of *citC* and *citM* overexpression on citric acid secretion in *P. fluorescens* PfO-1 harbouring NADH insensitive *cs*

Overexpression of *citC* in *Pf* (pY145F) strain caused both qualitative and quantitative changes in citric acid levels and yields. *citM* does not cause any significant difference in citric acid levels and yields when compared to *Pf* (pY145F) without any external citrate transporter.

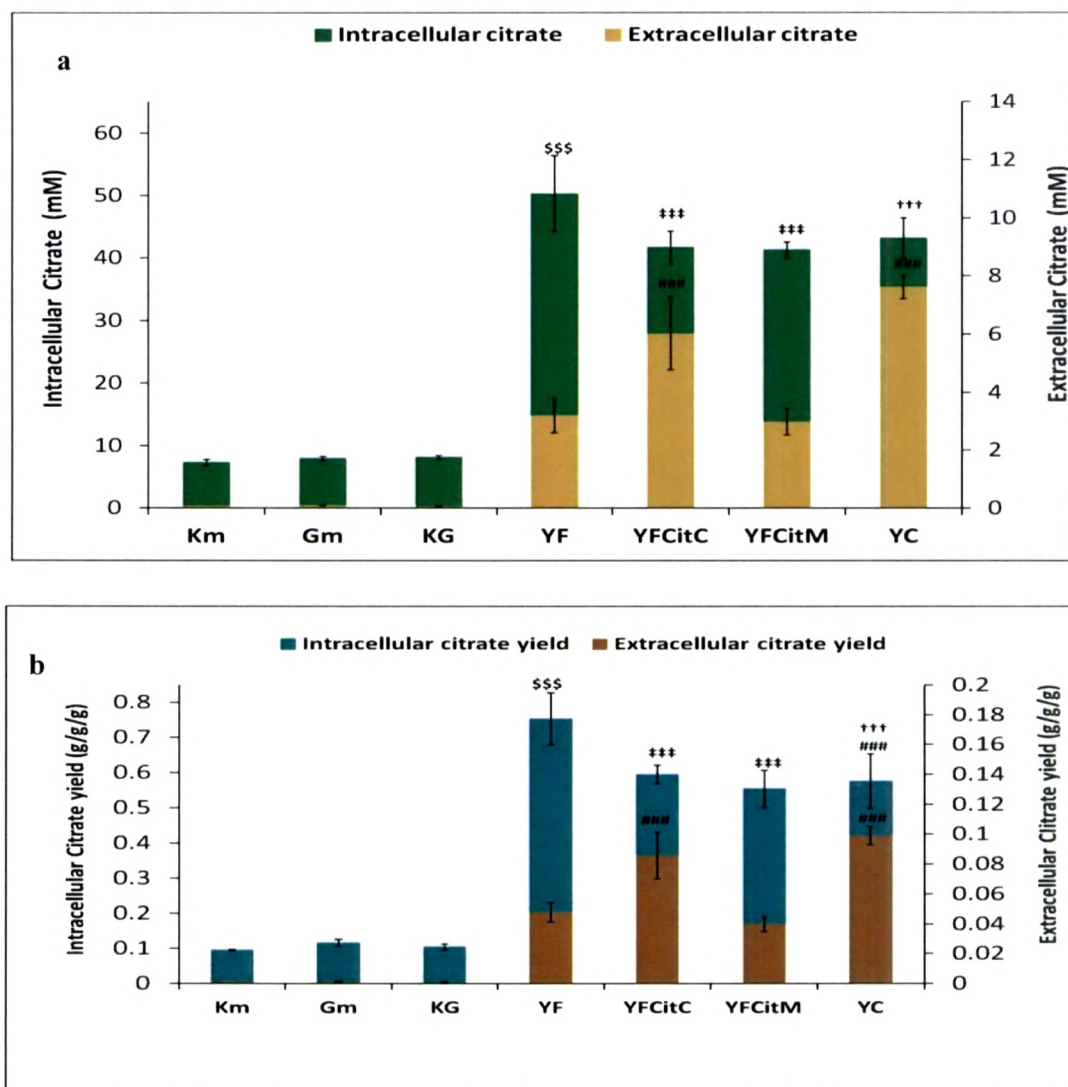


Figure 4.22 : Citric acid levels and yields in *P. fluorescens* PfO-1 overexpressing citrate transporter. Intracellular and extracellular citrate levels (a) are represented in green and orange bars

respectively. Intracellular and extracellular citrate yields are represented in blue and magenta bars respectively. Organic acid yields were estimated from stationary phase cultures grown on M9 medium with 100mM glucose and are expressed as g/g of glucose utilized/g dry cell mass. Results are expressed as Mean \pm S.E.M of 4 independent observations. \$ comparison of parameters with vector control Km, † comparison of parameters with vector control Gm, ‡ comparison of parameters with vector control KG, # comparison of parameters YF and YFCitC, YF CitM and YC. \$\$\$, †††, ‡‡‡, ###, P<0.001; \$\$, ††, ‡‡##P<0.01; \$, †, ‡, #P<0.05

Extracellular citric acid levels in *Pf*(pYFCitC) and *Pf*(pYC) increase by 1.88 and 2.3 fold as compared to *Pf*(pY146F) which is 92.6 and 84.6 fold higher as compared to vector control strain respectively. Corresponding extracellular citrate yield increased by 1.79 and 2.07 fold with an increase of 103.4 and 76 fold compared to respective vector controls (**Fig. 4.22**). Although there is an approximately 1.26 fold decrease intracellular citrate yield amongst the citrate transporter bearing strain this is not statistically significant. All experiments were further continued with *Pf*(pYC) and *pf*(pGm) as control.

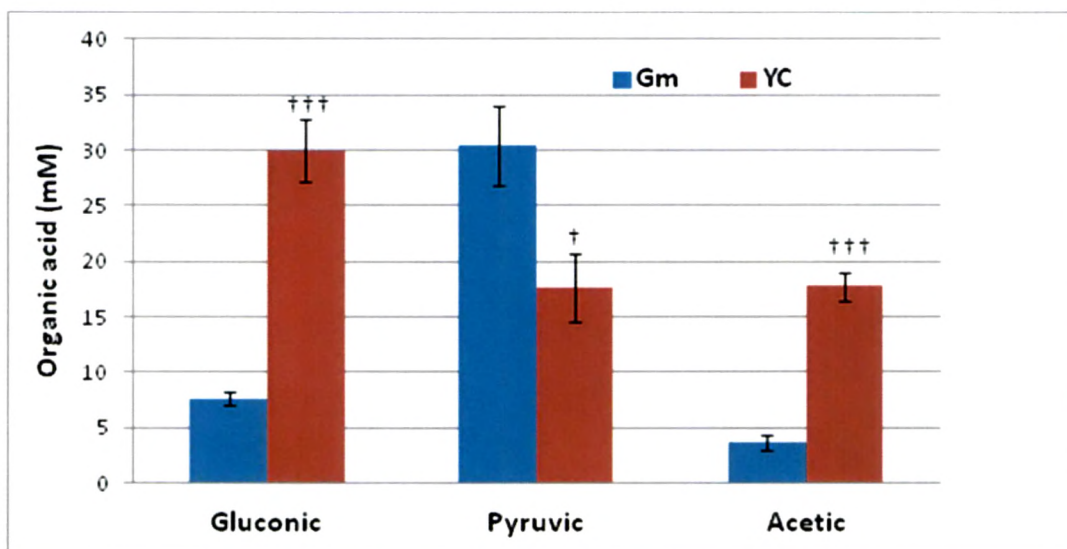


Figure 4.23: Organic acid secretion from *P. fluorescens* Pf0-1 overexpressing citrate transporter. Gluconic, pyruvic and acetic acid levels (mM) were estimated from *Pf*(pYC) with respect to control strain *Pf*(pGm) designated as respective colours in the graph. Parameters estimated from stationary phase cultures grown on M9 medium with 100mM glucose. Results are expressed as Mean \pm S.E.M of 4 independent observations. †Comparison with respect to pGm †††P<0.001; ††P<0.01; †P<0.05.

The YF-CitC overexpression caused quantitative changes in secretion of gluconic, pyruvic and acetic acid levels. Stationary phase culture supernatants of *Pf* (pYC) showed 3.91 and 4.81 fold elevated gluconic and acetic acid levels, respectively, and 1.73 fold decreased pyruvic acid level as compared to *Pf*(pGm) (Fig. 4.23).

4.4.6 Alterations in G-6-PDH, CS, ICDH, ICL, PYC, and GDH activities

In *Pf* (pYC) the periplasmic GDH activity increased by 1.46 fold as compared to the *Pf* (pGm) in late log to stationary phase of growth. Similarly a significant increase in G6PDH, PYC and CS activities by 1.46, 4.74 and 4.5 fold, respectively, were observed as compared to the controls. However, ICL and ICDH activities in the stationary phase cultures remained unaltered (Fig. 4.24).

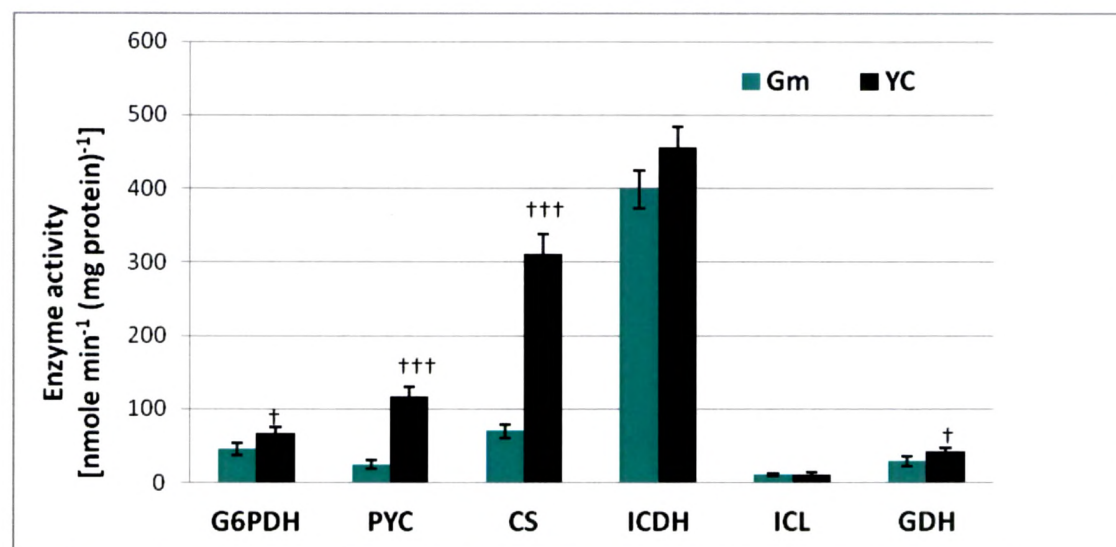


Figure 4.24: Activities of enzymes G-6-PDH, ICDH, ICL, PYC, and GDH in *P. fluorescens* PfO-1 overexpressing citrate transporter. The activities have been estimated using *Pf* (pYC) and vector control *Pf* (pGm) cultures grown on M9 minimal medium with 100mM glucose. All the enzyme activities were estimated from mid log phase and stationary phase cultures except ICL and GDH which were estimated only in mid log and stationary phase respectively. All the enzyme activities are represented in the units of nmoles/min/mg total protein. The values are depicted as Mean \pm S.E.M of 4 (N=4) independent observations. †Comparison with respect to pGm †††P<0.001; ††P<0.01; †P<0.05.

4.4.7 Effect of *citC* overexpression on growth, biomass and glucose utilization of *P. fluorescens* PfO-1

In the presence of excess glucose, increase in CS activity did not significantly affect growth profile and acidification of the medium within 30 h. However, there is a significant pH drop was found in case of *Pf* (pYC) compared to wild type and control strain. Specific growth rate, specific total glucose utilization rate after 30h remained unaffected. Total amount of glucose utilized increased by 1.44 fold and glucose consumed intracellularly is reduced by 1.27 fold in *Pf* (pYC) as compared to *Pf* (pGm). The increase in CS activity in *Pf* (pYC) strain improved the biomass yield by 2.58 fold compared to *Pf* (pGm) (Table 4.6, Fig. 4.25).

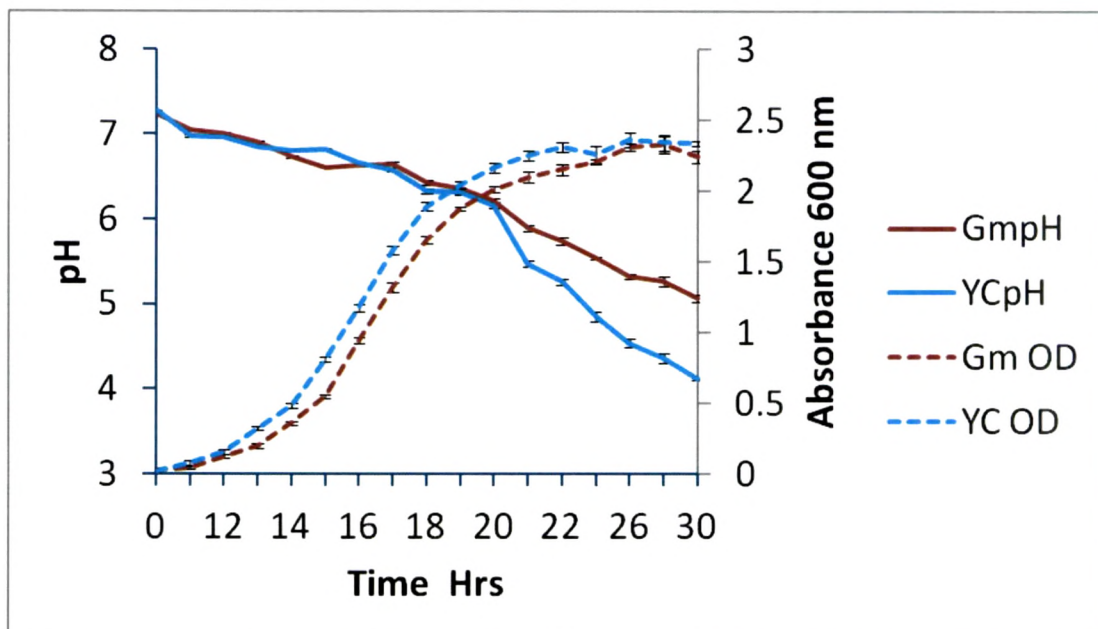


Figure 4.25: Growth and pH profiles of *P. fluorescens* PfO-1 pYC and pGm transformants on M9 minimal medium with 100mM glucose. The values plotted represent the Mean±S.D of 4-6 independent observations.

Table 4.6: Physiological variables and metabolic data from *P. fluorescens* Pf0-1 pYC and pGm transformants grown on M9 medium with 100mM glucose

Bacterial strain	Sp. Growth rate μ (h ⁻¹) ^β	Total glucose utilized(mM) ^ε	Glucose consumed (mM) ^ε	Biomass yield Y _{dcw/Glc} ^β (g g ⁻¹)	Sp. Glucose utilization rate Q _{Glc} ^β [g (g dcw) ⁻¹ h ⁻¹]
<i>Pf</i> (pGm)	0.52±.006	54.23±4.76	46.54±4.49	0.12± 0.031	6.6±0.85
<i>Pf</i> (pYC)	0.53±0.02	67.47±6.97 †	37.52±7.59 †	0.31± 0.053††	7.01±0.45

The results are expressed as Mean ± S.E.M of readings from 4-6 independent observations. ^β Biomass yield (Y_{dcw/Glc}), specific growth rate (μ) and specific glucose consumption rate (Q_{Glc}) were determined from the mid-log phase of each experiment. ^εTotal glucose consumed and glucose utilized were determined at the time of pH drop (30h) for *Pf* (YC) and control strain *Pf* (Gm). †Comparison with respect to pGm †††P<0.001; ††P<0.01; †P<0.05

4.4.8 Phosphate solubilization phenotype by *P. fluorescens* PfO-1 transformants harboring pYC plasmid expressing NADH insensitive *cs* and *S. tphilum* *citC* gene under *plac*.

PfO-1 (pYC) showed an improved MPS phenotype over PfO-1(pGm) in both PVK agar and TRP agar medium (**Fig. 4.26**).

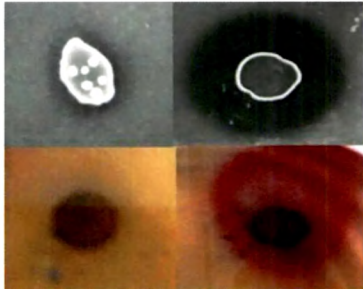
Strain	Zone diameter(cm)	
<i>Pf</i> (pGm)	0.69±0.05	
<i>Pf</i> (pYC)	1.62±0.23††	

Figure 4.26: Diameter of zone of clearance and colouration formed by fluorescent pseudomonad transformants on Pikovskaya's agar and tris rock phosphate agar containing 75mM glucose and 75 mM

Tris HCl pH 8.0. The results were noted after an incubation of 120 h at 30 °C and are given as mean \pm S.D. of three independent observations. † as compared to control Pf(pGm), †††<.001, ††<.01 and †<.05.

4.5 Discussion:

The present study demonstrates heterologous overexpression of *S. tephimurium* Na⁺ citrate and *B. subtilis* Mg²⁺ citrate transporter in citric acid secretion by metabolically distinct *P. fluorescens* PfO-1. Approximately 85 fold increases in extracellular citrate level compared to vector control *Pf* (pGm) and 2.5 fold as compared to *Pf* (pY145F with endogenous transporter) were achieved in the present study due to *CitC* overexpression. Considering the high amount of intracellular citrate accumulation after overexpression of NADH insensitive *cs* Y145F, the extracellular levels were relatively low suggesting that the endogenous citrate transporter (H⁺ citrate) was inefficient. An efficient transport system for citrate secretion was considered to be rate limiting in case of yeast (Anastassiadis and Rehm, 2005) while in addition to citrate transport, transport of sugar and ammonia into the cell was important for citrate production in *A. niger* (Papagianni, 2007).

The CitM transporter from *B. subtilis* transports citrate as a complex with Mg²⁺. Functional expression and characterization of *B. subtilis* CitM in *E. coli* DH5 α is reported in many studies (Boorsma et al., 1996; Li et al., 2002). In the present study, *citM* gene overexpression in *P. fluorescens* PfO-1 harbouring NADH insensitive *cs* gene does not lead to enhanced extracellular citrate level. *citM* gene expression is induced when citrate is present in the growth medium (Warner 2000; Blancato 2006). The expression of *citM* gene is under the strict control of the medium composition and carbon catabolite repression. In a similar manner, *citM* gene is also inducible by citrate and repressed by glucose in *B. subtilis* (Bergsma et al., 1983; Boorsma et al., 1996).

Increased gluconic acid levels with simultaneous reduction in pyruvic acid levels could be explained by increased PYC activity in *Pf* (pYC), which could probably divert pyruvate flux towards increased OAA biosynthesis to meet the increased CS activity. Even in *A. niger* the enhancement of anaplerotic reactions replenishing TCA cycle intermediates

predisposes the cells to form high amounts of citric acid (Legisa and Matthey, 2007). However, similar increase in flux through glyoxylate shunt was not apparent in *Pf* (pYC) as evident from very low and unaltered ICL activity detected in *Pf* (pGm) and *Pf* (pYC). Low ICL activity was consistent with earlier reports in *P. fluorescens* ATCC13525 and *P. indigofera* in which ICL contributed negligibly to glucose metabolism (Buch et al., 2009; Diaz-Perez et al., 2007).

Enhanced CS activity in *Pf* (pYC) also increased the periplasmic glucose oxidation which is reflected by increase in GDH activity and gluconic acid production. Significant increase in G6PDH activity is monitored in *Pf* (pYC). Significant decrease in glucose consumption and increase in total glucose utilization accounts for the carbon flux distribution in *P. fluorescens* PfO-1. The increased carbon flow through glycolysis led to increased protein synthesis that is reflected to increased biomass. The citrate induced oligosaccharide synthesis was reported in *Agrobacterium* sp. ATCC 31749 (Ruffing et al., 2011).

The summary of the result is depicted in the **Fig. 4.27**.

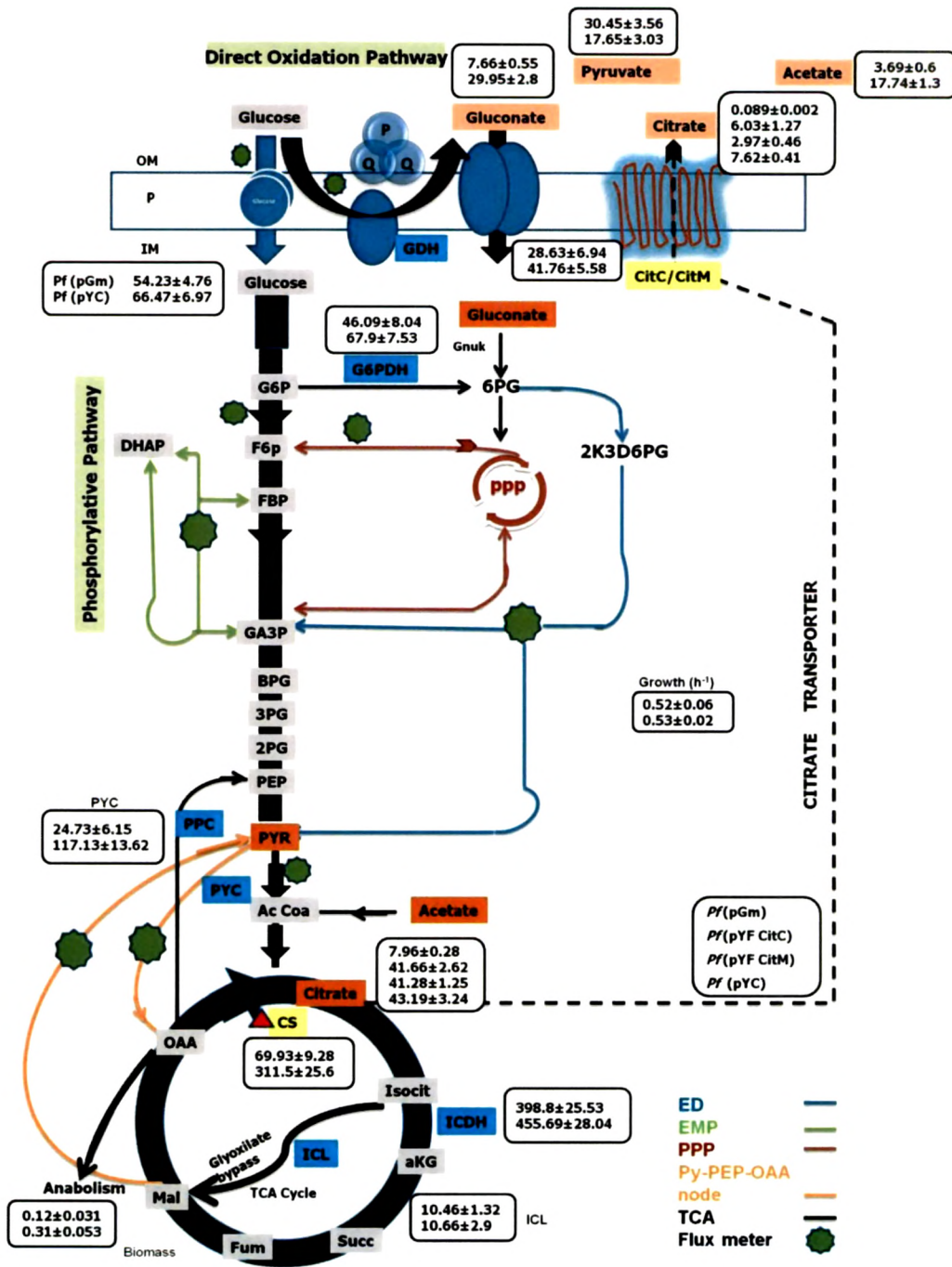


Figure 4.27: Key metabolic fluctuations in *P. fluorescens* PfO-1 overexpressing NADH insensitive *E. coli* CS and *S. thimurium* Na⁺ citrate transporter